Antiquity 2026 page 1 of 18
https://doi.org/10.15184/aqy.2026.10340

Research Article

Mediterranean maritime visibility: old limits and new approaches

Karl Smith & Linda Hulin

Institute of Archaeology, University of Oxford, UK
Author for correspondence: Karl Smith ✉ karl.smith@arch.ox.ac.uk

Much work on the archaeology of nautical mobility across the Mediterranean Sea draws on calculations of land visibility that were formulated in 1901 and that have received relatively little critical evaluation. Here, the authors trace the use of this map in archaeology, providing a critique of 2D coastal visibility analyses and presenting a new analysis to quantify coastal visibility in angular terms. The resulting multidimensional visibility datasets (available as online supplementary material) form the basis for an updated coastal visibility map for the Mediterranean Sea, offering a platform for the exploration of more nuanced questions about seafaring and navigation.

Keywords: Mediterranean Europe, GIS, seafaring, navigation, viewshed

Introduction

When sailing in daylight without modern instruments, having a clear view of the coast and a good set of landmarks is the most reliable way to navigate. In the context of the ancient Mediterranean, archaeologists have frequently invoked the visibility of land from the sea in debating the particularities of sailed routes, or the navigability of coastlines (i.e. Vernet 1978; Chapman 1990; Cunliffe 2017; Calvo-Trias & Galmés-Alba 2025). Map-based analyses of Mediterranean visibility, however, are extraordinarily few. Most authors have relied upon a single map—an exploratory visibility analysis published in 1901 and introduced to archaeology in the 1970s (Henkel 1901; Schüle 1970, 1980). This map has been used mainly to contextualise Mediterranean seafaring, though it has

Received: 6 August 2025; Revised: 4 December 2025; Accepted: 18 January 2026

also been used to support arguments about the capabilities of ancient mariners (i.e. Aubet 2001; Tartaron 2013).

We present here a long-overdue critique of this 1901 map by tracing its origins, comparing it with other isovist maritime-visibility formulae and reproducing it using modern datasets and geographic information systems (GIS). We find important discrepancies between published isovist formulae, and between the original 1901 visibility limits and those determined by our reproduction. We also present a novel 3D GIS method for quantifying visibility in angular terms; specifically, the angle that land rises above the horizon, the angle defined by land along the horizon and the projective 'area' that land occupies in an observer's visual field. The scripts that we use for this analysis generate multidimensional outputs that allow us to test visibility using varying sea levels (i.e. tide heights) and maximum-visible-distance limits. We use these scripts to produce a Mediterranean-wide visibility analysis that provides new information about visibility *within* the 'visibility limit' established by older approaches.

This article demonstrates how maritime visibility—which we define as the degree to which landforms can be observed and recognised by an observer on a ship at sea—transcends the 'now you see it, now you don't' binary represented by a single line on a map. Filling in the gap between this line and the coast helps us better understand what ancient mariners would have experienced on their journeys and gives us a methodological framework for incorporating more complicated visibility factors, such as atmospheric effects, into our analysis. This analysis forms part of our ongoing work modelling maritime movement as part of The Practical Mariner project, and making our scripts and continuous visibility datasets openly available (see Smith 2026 and online supplementary material (OSM), respectively) will be useful for other researchers building models of ancient seafaring and marine landscapes.

Tracing Henkel's 'visibility limit' in archaeological scholarship

For half a century, archaeologists interested in maritime navigation in the Mediterranean Sea have turned to Wilhelm Schüle's map of "Grenze der Sichtbarkeit des Landes auf dem Mittelmeer" ("limit of visibility of land in the Mediterranean"; Schüle 1970: fig. 1, 1980: fig. 2). Although Schüle is credited in these publications as the originator of this map, it is in fact a duplicate of a 1901 analysis of Mediterranean and Aegean visibility by Ludwig Henkel (1901: fig. 1; see Figure 1). Schüle introduced Henkel's map and formula to archaeology first in a conference paper and later in the preface to a site monograph (Schüle 1970, 1980), describing his own map as a 'slightly simplified reproduction' of Henkel's. Since Schüle uses the same formula, references identical source data and replicates Henkel's anachronistic treatment of the Nile Delta (see below), we consider his map to be a direct copy of Henkel's (cf. Schüle 1970: 458–60; Henkel 1901: 285; see also Table 1).

Critical examination of the use of Henkel's map in archaeological analyses reveals how it has been used to support different 'expansive' models of maritime mobility—that is, models in which long-distance voyages were regular, frequent and/or easily accomplished. Henkel's original formulation was itself inspired by a curiously anthropomorphic view of prehistoric seafaring. In the introduction, Henkel (1901: 284) cites as his

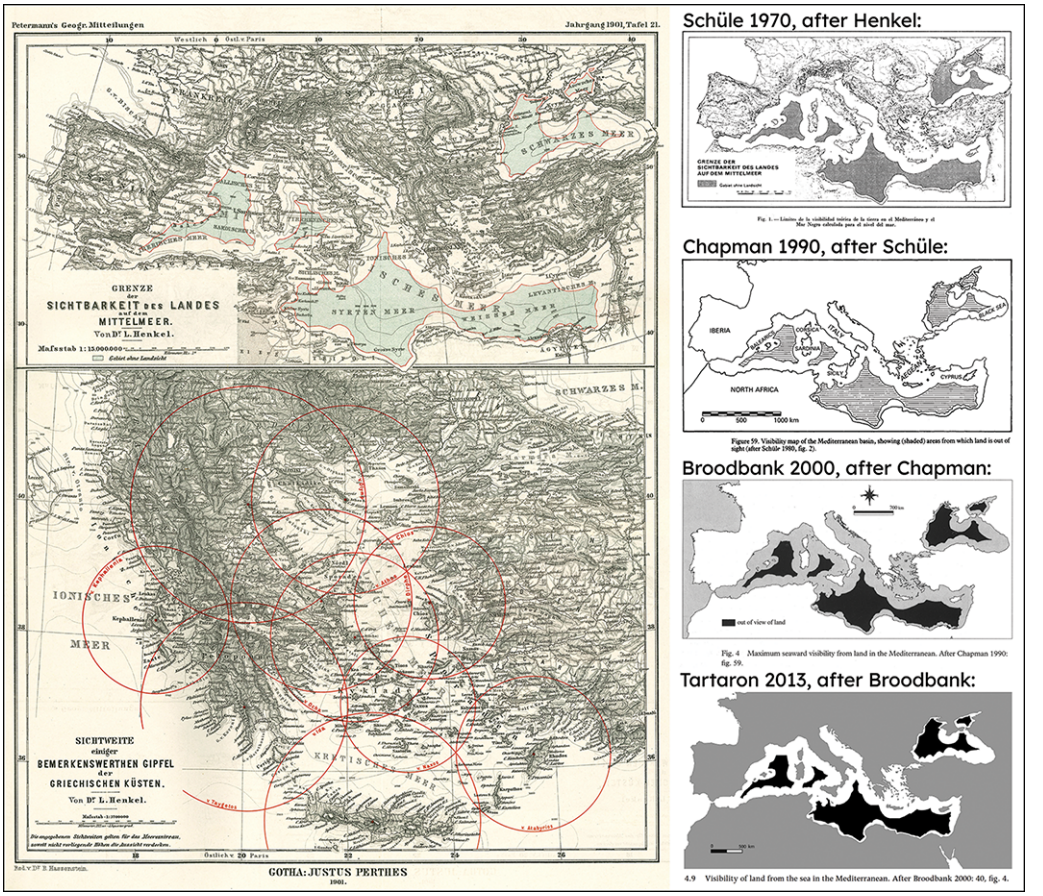

Figure 1. Henkel's map of Mediterranean visibility/isovists for selected mountain peaks in the Aegean (left; 1901: fig. 1), and selected reproductions of Henkel's map (right) (figure by Karl Smith; © The Practical Mariner).

inspiration Neumann and Partsch's *Geographie von Grieschenland*, which he claimed contained "perhaps the most beautiful" description of the use of landmarks in ancient navigation:

> *If this advantageous design of their coast made it a game for the Greeks to venture out onto the water, they were irresistibly lured from the quiet bays to the high seas by the sight of land everywhere in the short distance … And once this step had been taken, one station point led to the next; densely packed in the Greek Sea were landmarks of the most excellent kind … The sailor never felt alone between sky and sea: he always had a coast before him, which, if the wind and weather were not too adverse, he could reach by rowing in a few hours* (Neumann & Partsch 1885: 146–47; authors' translation).

Henkel uses similar framing in claiming that his map shows how "the Carthaginian sailor never lost sight of land on his voyages to Sardinia or Sicily, as the islands of Galite

Table 1. Published isovist formulae.

Publication	Formula*	If $E_m = 500$, $D_{km} =$	*If* $E_m = 3400$, $D_{km} =$
Henkel 1901: 458	$D_{km} = 3.8 * \text{sqrt}(E_m)$	84.97	221.58
Inman 1920: ix	$D_{nm} = 1.15 * \text{sqrt}(E_{ft})$	86.26	224.94
Schüle 1970: 458; 1980: 16	$D_{km} = 3.8 * \text{sqrt}(E_m * 1000)$ **	2687.01	7006.85
Vernet 1978: 328	$D_{km} = 3.5696 * \text{sqrt}(E_m)$	84.48	208.14
Medas 2004: 75	$D_{nm} = 2.04 * (\text{sqrt}(E_m) + \text{sqrt}(O_m))$	84.48 if $O_m = 0$, 96.42 if $O_m = 10$	220.30 if $O_m = 0$, 232.25 if $O_m = 10$
Manning & Hulin 2005: 277 (and *pers. comm.*)	$D_{nm} = (1.17 * \text{sqrt}(E_{ft})) + (1.17 * \text{sqrt}(O_{ft}))$	87.76 if $O_m = 0$, 100.17 if $O_m = 10$	228.85 if $O_m = 0$, 241.27 if $O_m = 10$

*D_{units} = visible distance; E_{units} = land elevation; O_{units} = observer height; nm = nautical miles.

**Schüle's addition of the '1000' term likely resulted from confusion over unit conversions. His example "11.4 = 3.8* sqrt(9 * 1000)" (1980: 16) is only correct if the '1000' term is removed, in which case the formula is identical to Henkel's.

and Pantellaria guided him across" (1901: 284–85; authors' translation). For these authors, the long-distance visibility of landforms enabled—perhaps even motivated—prehistoric voyages.

Schüle, meanwhile, approached maritime mobility mainly as a mechanism to explain the movement of archaeological material around Mediterranean shores, arguing that similarities between artefacts in areas connected by the sea suggested direct, long-distance contact (see citations in Schüle 1980: 17). While contemporary scholars, such as Bowen (1970), used distribution maps to support their maritime theories, Schüle turned to Henkel's visibility map:

> *. . . of all the islands in the Mediterranean, there is not a single one that cannot be seen before leaving the visibility of the coast or the visibility of another island that has this quality . . . the nautical difficulties of this voyage are minimal compared to those that Polynesian sailors used to overcome less than a century ago* (Schüle 1970: 461–62; authors' translation).

Arguments similar to Schüle's have been voiced more recently by Aubet (2001: 168), who supports her argument that Phoenicians must have made long-distance overnight voyages by claiming (audaciously) that "it has been proved that in favourable weather conditions, with very few exceptions, the coast or the mainland is visible from any point in the Mediterranean" in reference to Schüle's map. Tartaron (2013: 108–109) also uses Henkel's map in support of an argument that long-distance offshore navigation was possible throughout the Mediterranean, except between Crete and Libya. Other authors use Henkel's map to suggest areas that navigators may have preferred or avoided, without arguing that the map supports a particular theory of Mediterranean mobility (Chapman 1990: fig. 59; Cunliffe 2008: fig. 212, 2017: fig. 2.4; Calvo-Trias & Galmés-Alba 2025: fig. 1). The remaining appearances of Henkel's map in archaeological literature use it to provide general context for their maps of the Mediterranean (Broodbank 2000: fig. 4, 2015: overleaf; Horden & Purcell 2000: fig. 9; Höckmann 2005: fig. 1).

Unfortunately, most archaeological reproductions of Henkel's map are confused about or indifferent to its provenance. Many of the aforementioned works do not cite any source for the map, or else cite a source other than Henkel or Schüle. For example, Tartaron's (2013) version of Henkel's map is attributed to Broodbank (2000), who attributes it to Chapman (1990), who attributes it to Schüle (1980) (see Figure 1). This confusion is probably one of the reasons why Henkel's 'visibility limit' has escaped criticism despite its widespread use in archaeological analyses. None of these cited authors have attempted to evaluate Henkel's method on its own terms—as a spatial analysis—or presented arguments for or against its application to archaeological problems.

Evaluating Henkel's 'visibility limit'

Henkel's map is based on a simple formula: the distance (in kilometres) within which a point on land should be visible is equal to 3.8 multiplied by the square root of the point's elevation (in metres; see Table 1). Henkel produced his map by applying this

formula to 62 mountain peaks spread throughout the Mediterranean littoral (Henkel 1901: 285). This method can be described in modern GIS terms as merging 2D buffers to create a visibility isoline, or 'isovist' (see Benedikt 1979; Lonergan & Hedley 2016). Unlike architectural isovists, which show the theoretical limits of visibility from a particular point, Henkel's formula produces an isoline that represents the limits of visibility of a set of points. However, Henkel did not apply his formula consistently; for the Nile Delta, he replaced his isoline with a 20-nautical-mile buffer (representing the visible distance of lighthouses), because "otherwise [the visibility limit] would run close to the flat shore" (Henkel 1901: 285; authors' translation). He also did not provide a source for his formula in his 1901 paper but did express hope that it would "stimulate observations [of] the extent to which practical visibility corresponds to theoretical visibility" (Henkel 1901: 285; authors' translation).

Henkel's formula is one of several similar formulae published by archaeologists (compared in Table 1). McGrail (1998) published an isovist formula in 1987, which he attributes to the 1920 edition of Inman's *Nautical tables* (Inman 1920, ix). McGrail (1998: 278) describes this formula as an "approximation [of] theoretical distances from sea-level", noting that "in meteorological conditions of refraction high ground may be seen at more than the theoretical distance. In poor visibility the distance is much less". Vernet (1978: 328) independently derived his own visible-distance formula, which includes a variable for observer elevation above sea level. Vernet's paper is probably the source or inspiration for Medas's (2004: 75) isovist formula, applied to Mount Etna (Medas cites Schüle, McGrail and Vernet; but Table 1 shows his results agree with Vernet). Medas's formula has been used recently in visibility analyses by Calvo-Trias and Galmés-Alba (2025: 272–74), which include isovists as a component in GIS visibility analyses of the Baleares. A final isovist formula was independently developed by Manning and Hulin (2005: fig. 1), whose equation also takes observer height into account. Their map of visibility in the Eastern Mediterranean is reproduced by Cunliffe (2017: fig. 3.9), with the visibility limit blurred so as not to suggest a hard cutoff.

Publications that cite Henkel or Schüle do not critique Henkel's method, input data or results, and typically focus on regions of the Mediterranean rather than the entire basin. We therefore provide an evaluation of Henkel's data sources and method—specifically, his reliance on isovists based on a small set of mountain peaks (and lighthouses)—by reproducing his map in GIS. We based our reproduction on Henkel's formula and the *GMTED2010* global 15-arcsecond digital elevation model (DEM; see Danielson & Gesch 2011). For each cell in the DEM, we constructed a buffer in ESRI ArcGIS Pro 3.6 using Henkel's formula and merged these buffers to generate the isovist shown in Figure 2.

Initially, our isovist appears to be similar to Henkel's. At a Mediterranean-wide scale it is slightly more conservative: the total 'out of sight of land' area defined by our model is approximately 1.6 per cent larger than Henkel predicts. However, focusing on specific areas reveals larger discrepancies. For example, we have not reproduced Henkel's decision to base his isovist on lighthouses rather than mountain peaks in the Nile Delta. As such, the distance between ours and Henkel's isovist is approximately 20–40km in the delta, with our results suggesting (as Henkel suspected) that the delta would have been

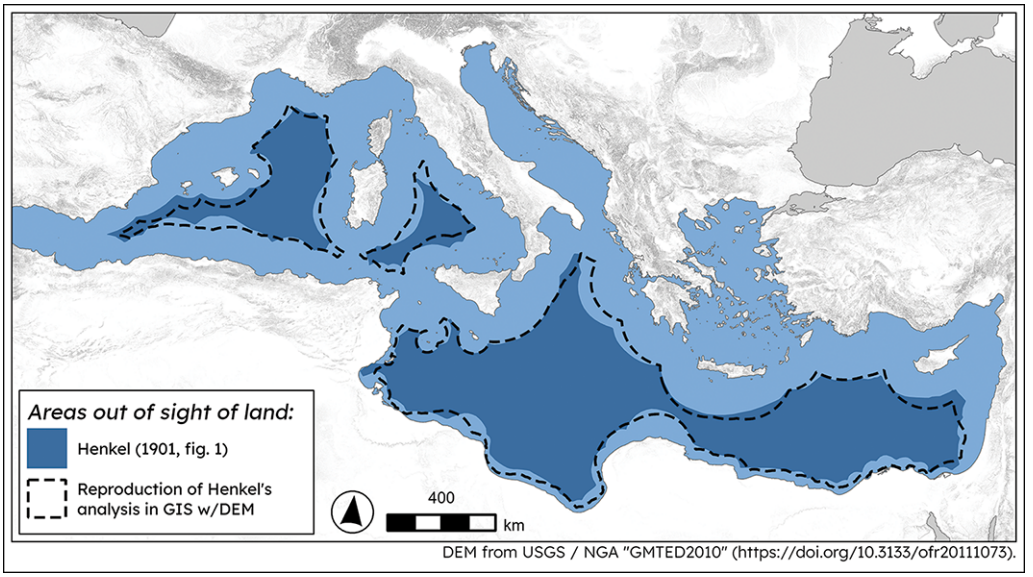

Figure 2. Map comparing Henkel's 1901 isovist (dark blue) with our GIS reproduction (dashed line) (figure by Karl Smith; © The Practical Mariner).

visible only within 5–10km of the shore. There are also large distances between ours and Henkel's isolines in the Black Sea, off the west coast of Greece, the north coast of the Italian island of Ustica, the east coast of Sardinia and the south coasts of Cyprus and the Baleares. In all cases the furthest distance between the two isolines is 35–50km. On the other hand, both models confirm Henkel's (1901: 258) assertion that land ought to be visible from anywhere within the Aegean and Adriatic. Additionally, both models suggest that it is possible to maintain sight of land while sailing between the Baleares and the mainland, between Sardinia and Africa, and between Cyprus and the Levant.

These comparisons illustrate how the application of Henkel's method can be improved by using all cells in a DEM rather than a small number of topographic prominences/lighthouses. We can also critique isovist formulae on a theoretical level by comparing them directly. Table 1 demonstrates that, because published isovist formulae have exponential terms, plotting the results of these functions for a range of land elevations results in a set of curves that grow further apart as elevation increases. For example, the difference between the greatest and least 'visible distance' values produced by these formulae for a point 500m high is 1.78km, but the same difference for a point the height of Mount Etna (approx. 3400m) is 20.72km. The same effect technically applies to the observer-height terms in Medas's and Manning and Hulin's formulae, but the smaller range in plausible viewing elevations makes the difference negligible. To the best of our knowledge, these observations constitute the only published comparative analysis of these isovist formulae. We believe that these theoretical methods should be confirmed by experiment (in the field or in GIS) before isovist formulae are accepted as valid methods for estimating the visibility of land.

Considering viewshed-based approaches to maritime visibility

The most obvious GIS alternative to an isovist-based approach to the maritime visibility of land would be a viewshed-based approach. The viewshed algorithm is a widely used GIS technique for quantifying visibility (for example: Wheatley & Gillings 2000; Llobera 2003; Brughmans *et al.* 2018), which tests observer-target sight lines against a raster elevation surface—if a sightline is obstructed the cell is marked as 'not visible', and if it is unobstructed the cell is marked as 'visible' (see Fisher 1993). Viewsheds can be combined to create 'cumulative' visibility analyses (in the context of seafaring, see Gillings 2009; Gustas & Supernaut 2017; Calvo-Trias & Galmés-Alba 2025). The only direct archaeological critique of Henkel's map (or, more precisely, of Aubet's 2001 reproduction) is Čučković's (2016, 2018) cumulative viewshed analysis for the Mediterranean using the Quantum GIS plug-in for QGIS. In his analysis, the value in each cell of the image represents the results of a viewshed with an observer in that cell. Čučković used 50km and 150km distance-bands to simulate visibility under different conditions, and it is telling that these bands are parameters, not products, of his model. This is necessary because viewsheds are designed primarily to quantify obstruction—the results of a single viewshed are not sensitive to changes in the relative positions of observer and target, except insofar as that change in position increases or reduces the target features' visible area. To illustrate why this distinction is especially important in a maritime setting, consider the following hypothetical situations (illustrated in Figure 3).

Imagine you are floating in the sea 5km off the shore of a small island. The island is conical, has a diameter of 2km and rises 1km above sea level. In this scenario the sea is a flat plane, so the angle between your horizon and the highest visible point of the island can be calculated by taking the arctangent of the island's elevation divided by the

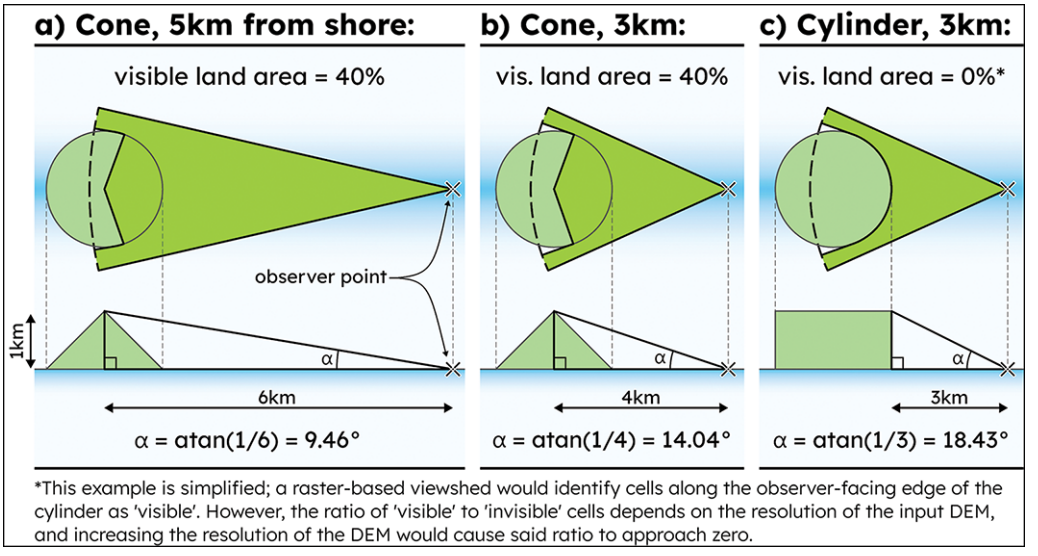

Figure 3. A comparison of the results of viewshed (in plan, top) and angular visibility measurement (in section, bottom) on idealised landforms seen from the sea (figure by Karl Smith; © The Practical Mariner).

distance from the observer to the island's centre—in this case 0.165 radians or 9.45° (Figure 3a). On the other hand, if the island is perfectly conical a viewshed will tell you that about 40 per cent of the cone's area is visible. Now sail 2km towards the island and go for another swim. Using the arctangent formula, you calculate that the island's angle-above-horizon increases from 9.45° to 14.04° (Figure 3b). Meanwhile, at a distance of 3km our perfectly conical island will remain 40 per cent visible according to the viewshed. Finally, imagine that the island is cylindrical instead of conical (Figure 3c; in a more realistic scenario it might be surrounded by cliffs). From your vantage point 3km off the shore the island's angle-above-horizon increases to 18.43°, because the upper rim of the cylinder is closer to you than the island's centre. But because the edge of the cylinder now obstructs your view of the top of the island, the island's 'visible area', according to a viewshed, drops from 40 per cent to a negligible percentage (for details, see Figure 3c).

These thought experiments illustrate two important points. First, 'visible area' defined by a viewshed does not necessarily increase or decrease as an observer moves towards or away from the target, provided that the target is regularly-shaped and there are no intervening obstacles. Second, viewsheds will fail to recognise as 'visible' features defined by cliffs when an observer is at the cliff base. In both cases, using angular measures fits our basic assumptions about visibility (land should be more visible when closer; larger landforms should be more visible than smaller landforms), while measurements of visible area produce counterintuitive results. These limitations have been highlighted in terrestrial viewshed applications (i.e. Wheatley & Gillings 2000: 25), but in a maritime context they are much more difficult to excuse.

Building a 3D visibility model

Given the limitations of the isovist and viewshed approaches to the visibility of land from the sea, we developed a 3D GIS method for measuring the visibility of land in angular terms using Python and ESRI ArcGIS geoprocessing tools. This technique follows 3D approaches to landscape and 'coastscape' assessment (especially: Higuchi 1983; Jerpåsen 2009; Bernardini *et al.* 2013). Following Pouncett (2013), our scripts generate a radial array centred on an observer point, sampling points on that array to compute visibility indices (see Figure 4). We then generate a list of points at regular intervals along each ray, and adjust the elevation-values of these points to simulate Earth curvature (see Yoeli 1985: 92–93). Next, we check that these points are (1) unobstructed by other points along the ray, and (2) within a pre-set maximum visible distance. Upon completing this check, our script returns either an empty list (in which case no points along the ray are visible), or a list of visible elevations. Finally, we compute angular values for all visible elevation points using the arccosine function.

Using these lists, our scripts compute three angular visibility indices: maximum vertical angle, sum horizontal angle and total subtended area. These represent, respectively, the highest angle that land appears at over the horizon, the angle along the horizon occupied by land and the 'size' of land as it appears to a viewer. Maximum vertical angles are calculated by finding the maximum angular value for all rays in the radial

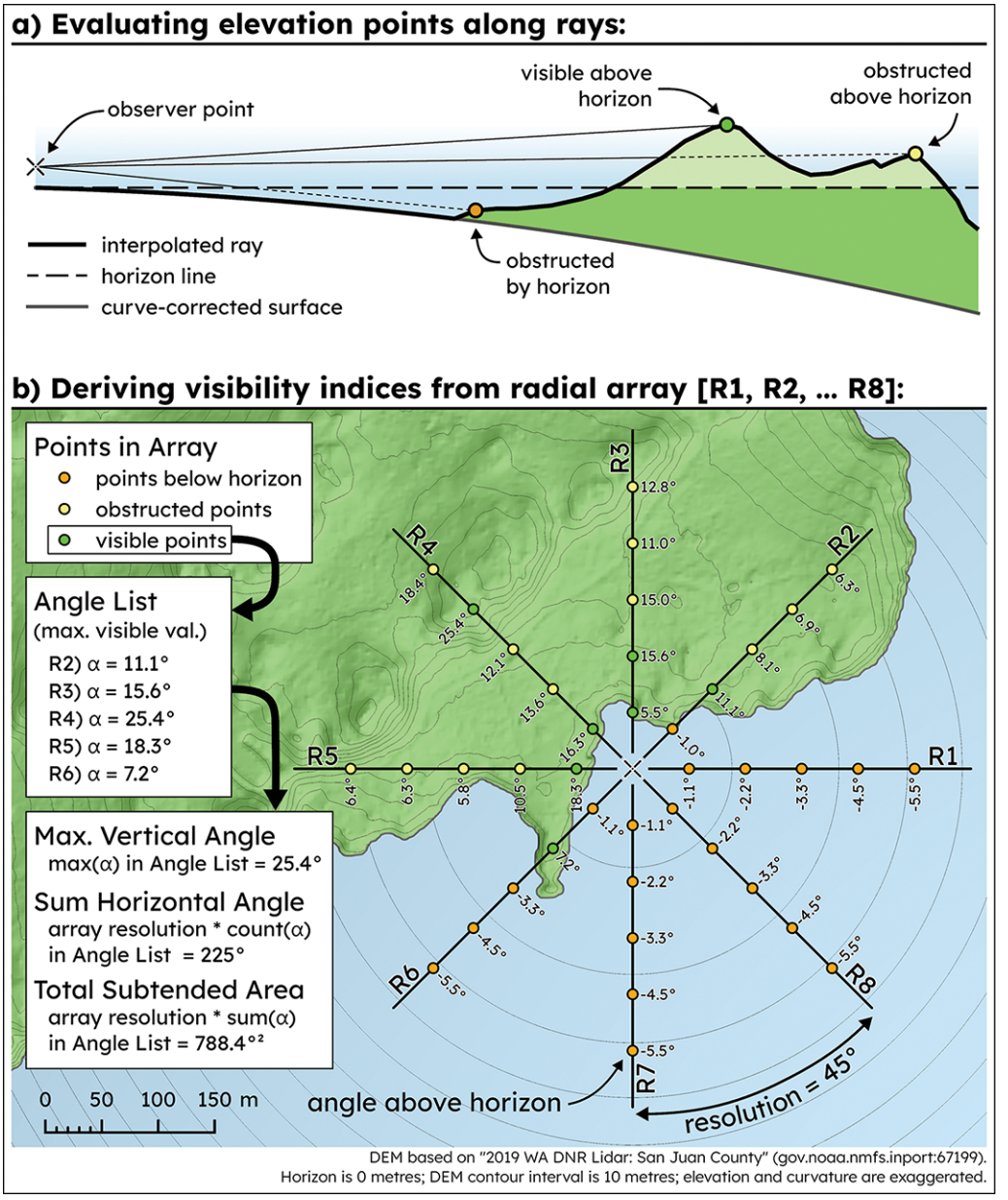

Figure 4. Illustration of the radial array method with elevation and curvature exaggerated, showing: a) curvature-correction and obstruction-checking for individual rays, and b) calculation of visibility indices for a simple array (figure by Karl Smith; © The Practical Mariner).

array. To compute the sum horizontal angle, our script multiplies the number of rays that return visible elevations by the angular resolution of the array. Finally, total subtended area is calculated by finding the maximum angular value for each ray in the array and multiplying the sum of these values by the array's angular resolution.

Our other scripts co-ordinate our visibility model over the following dimensions: latitude, longitude, sea level height and maximum visible distance. In the first two cases, every combination of latitude and longitude are tested for intersection with features representing land to obtain a regular grid of 2D points that are located at sea. A radial array is constructed for each point, and the process described above is completed for (1) a series of observer heights, and (2) a series of maximum visible distances. The final output of our script is a 5D array, stored as a NetCDF file (see Rew & Davis 1990). NetCDF is a flexible data format that stores variables (in our case: maximum vertical angle, sum horizontal angle and subtended area) at points along a set of dimensions (for us: x-coordinate, y-coordinate, water surface height, observer height and maximum visible distance). Using GIS/statistics software our 5D arrays can be queried to determine, for example, visibility values for certain points, or sliced/flattened to produce raster images. The figures presented in this article are subsets of our larger visibility arrays (see OSM).

A new Mediterranean maritime visibility map

We used our projective visibility scripts to perform an analysis for the Mediterranean for a 5km grid of points masked by the HydroSHEDS v.1 hydrological dataset (see Lehner *et al.* 2008). We used four tide heights, an observer height of 1.5m and a range of visible distances corresponding to weather types reported by the World Meteorological Organization (2009: A-351). Other variables used by the script and in our analysis can be found in Table 2. We imported the resulting NetCDF file into ArcGIS Pro and extracted data slices as rasters to create the figures in this article. Figure 5 shows angular measures derived from our model's output, classified into categories. Figure 5a shows that the outer limit of visibility defined by our model is broadly similar to our isovist. There are, however, some important discrepancies: our model contains areas 'out of sight of land' within the Adriatic and between Cyprus, the Baleares and their respective mainlands, and does not suggest that maintaining sight of land while sailing between

Table 2. Parameter inputs and data sources for our visibility model.

Parameter	Value/Source
Shore limits	*HydroSHEDS v1 (Lehner* et al. *2008)*
Elevation model	GMTED2010 *1-arcsecond DEM (Danielson & Gesch 2011)*
X/Y spacing	*5/5km*
Surface elevations	*Every half metre from −2m to 2m above sea level*
Observer height	*1.5m*
Distance ranges	*Every 500m from 500–5000m; every 1km from 5–40km; every 10km from 40–70km*
Radial array resolution	*1° (360 rays/point)*
Ray densification distance	*500m*

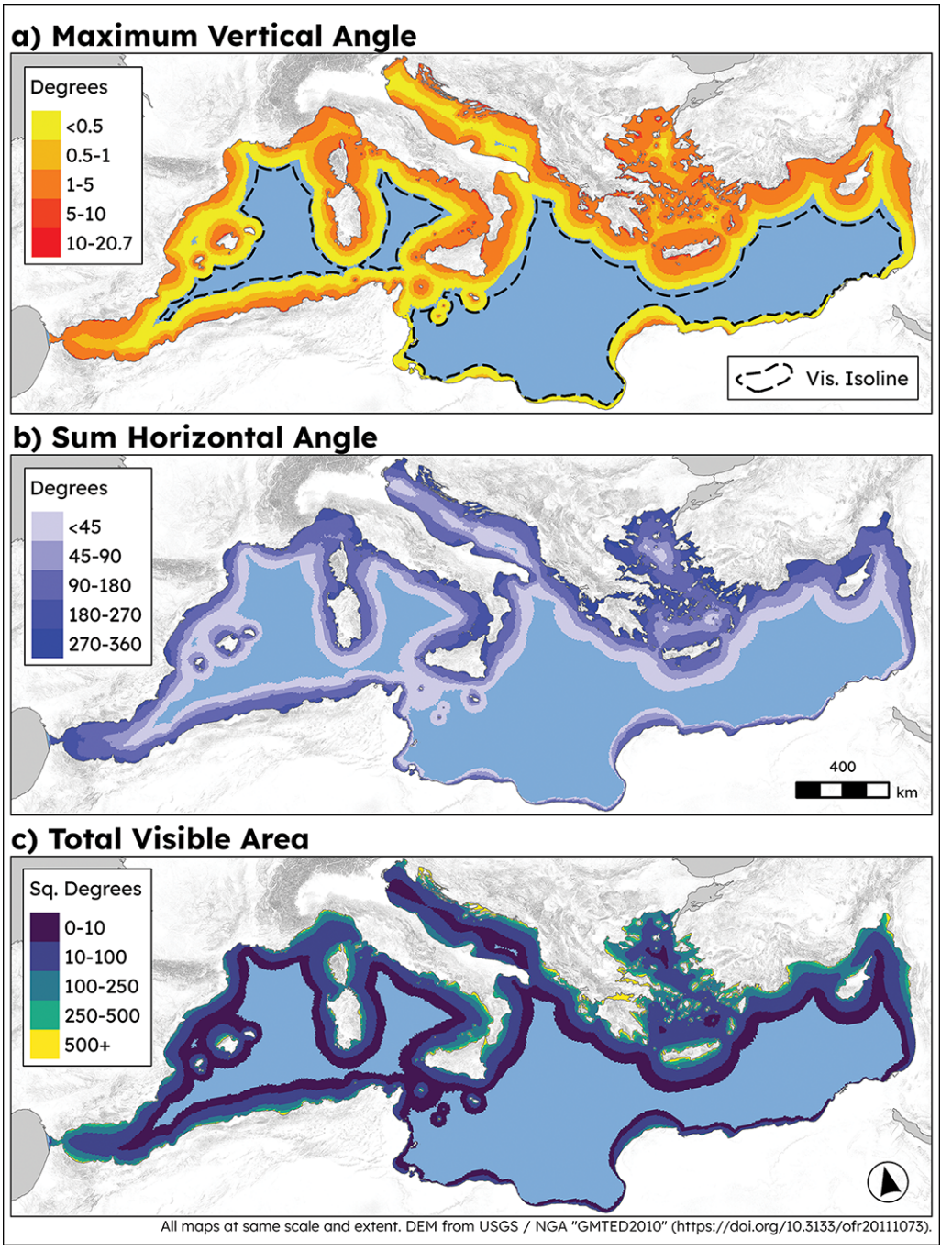

Figure 5. Classified results of the Mediterranean visibility model (figure by Karl Smith; © The Practical Mariner).

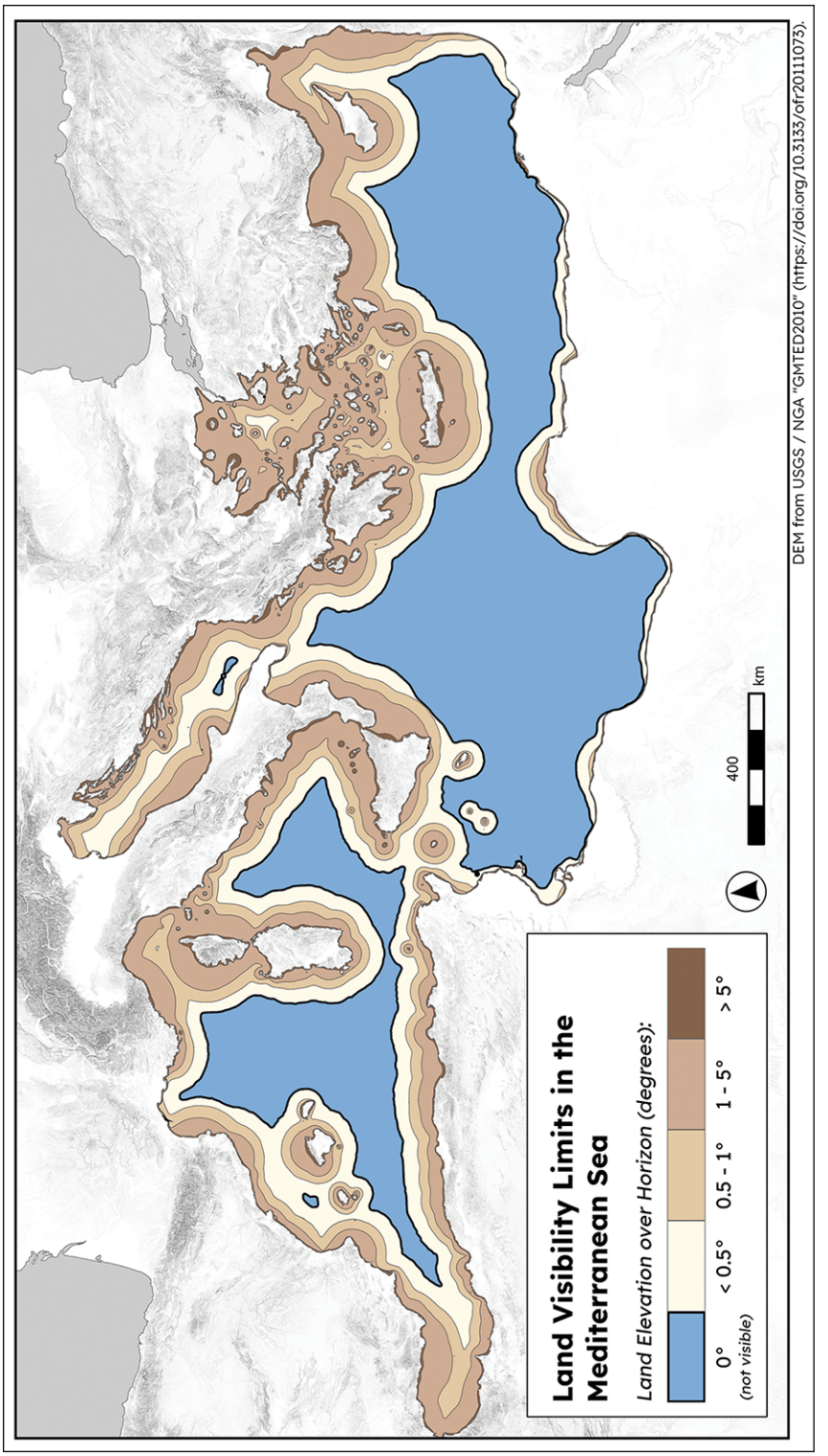

Figure 6. An updated visibility map for the Mediterranean (figure by Karl Smith; © The Practical Mariner).

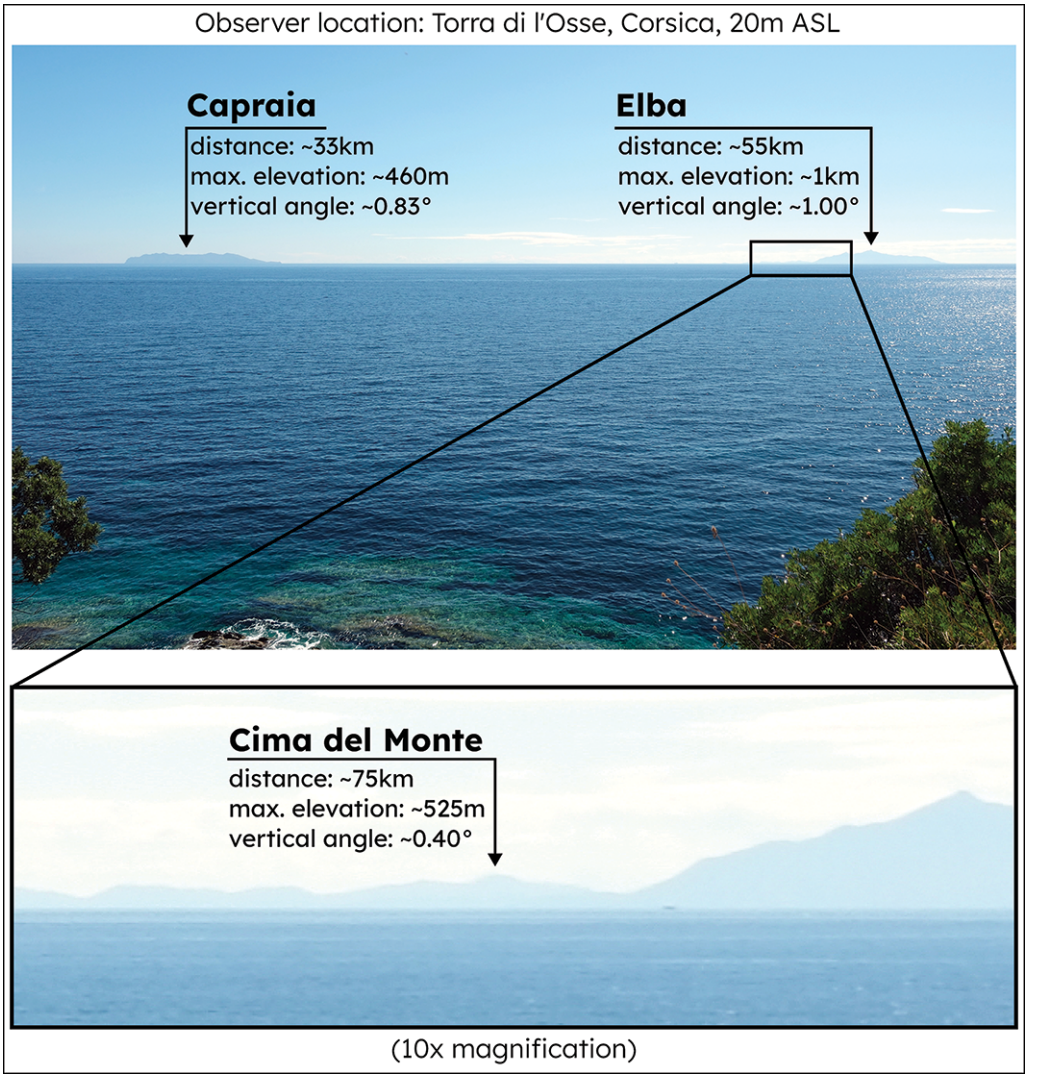

Figure 7. Maximum vertical angle measurements calculated for peaks on the islands of Capraia and Elba, viewed from Corsica, with magnified inset at bottom showing the same measurements for Cime del Monte, Elba (figure by Karl Smith; © The Practical Mariner).

Sardinia and Africa is possible. The values in Figure 5a are much lower than expected, only rising higher than 5° within 5–20km of the coast in most cases. The classified sum horizontal angle plot (Figure 5b) highlights 'enclosed' areas, where seafarers would have been able to see more land along the horizon—especially the Cyclades, Anatolia, the Dalmatian Coast and the straits of Gibraltar and Messina. In the case of Cyprus, it suggests that sailors approaching from the north would have stood the best chance of keeping land in view along the horizon. Finally, the classified total subtended area plot (Figure 5c) is a useful synthesis of the two other indices. It highlights visually prominent

coastlines like that of Crete and Sicily, as well as littoral areas that are relatively more visible, like the eastern Libyan coast.

We believe that of the three measures, the maximum vertical angle is the most directly comparable to isovist results and is also the easiest to understand intuitively. We therefore use this measure as the basis for our updated Mediterranean visibility map (Figure 6). To produce this map, we ran the ArcGIS 'Contour' tool on a slice of our unclassified maximum vertical angle dataset (for parameters used to define the slice, see the readme file in the OSM). The contours in this case represent the areas in which land can be seen at 0, 0.5, 1 and 5+° above the horizon. While the outer limits of visibility in our map are broadly similar to Henkel's, there is considerable variability within that outer limit. For example, our analysis suggests crossings from the Balkans to Italy, from Sicily to Africa, across the Gulf of Lion and from the Baleares to Europe would have involved traversing areas of the sea where land rises less than half a degree above the horizon. In fact, our models suggest that for most of the area within Schüle's 'visibility limit', land rises less than half a degree above the horizon. For reference, the width of your smallest finger held at arm's length is approximately one degree; Figure 7 shows three landforms that rise up to one degree above the horizon (as calculated by our Python scripts), viewed under good conditions. We believe that mariners without telescopes or night-glasses would find it difficult to identify landforms that rise less than half a degree above the horizon—especially in foul weather—even if land technically could be viewed.

Conclusions and future development

In reproducing Henkel's visibility map and building our own 3D analysis from first principles, we have made considerable advances in a line of inquiry that has received little attention from archaeologists over the past 125 years. The fact that isovist formulae have become, *de facto*, the standard method for quantifying large-scale Mediterranean visibility in antiquity demonstrates the need for more critical thinking about how visibility informs the experiences and decisions of Mediterranean mariners. For example, Schüle (1970: 461) acknowledges that visibility can be affected by bad weather but contends that seafarers would have avoided such conditions and that "it would be absurd to draw a visibility map of the coast in case of fog or mist" (authors' translation). In the context of the maritime movement models being developed by The Practical Mariner project, having datasets that represent visibility under different conditions is crucial—we contend that it is more absurd to assume that sailors in the Mediterranean were never unexpectedly fog-bound. The results of our 3D visibility analysis demonstrate how 'visibility' varies within the shore's 'visible limit'. Our results do not on their own overturn the theories of maritime movement espoused by the other scholars mentioned here, but we hope that they will serve as a caution to future theorists and an inspiration for the development of more nuanced analyses of maritime visibility. Researchers should confront the fact that visibility is contingent on dynamic factors like atmospheric scattering (i.e. the effects of dust, mist and fog), colour and light contrasts, and optical effects like refraction and wave reflection (see Jerlov 1976). The possibility of night sailing (and the

use of lights at night) also complicates the picture (Mauro & Durstante 2023). These are all factors that can be incorporated into future visibility models.

Atmospheric refraction, which can make land visible at greater distances (McGrail 1998: 278), was not included in our visibility model, and it is possible that our own map is too conservative about visibility as a result. We did not incorporate refraction into our model because atmospheric refraction is an optical effect that is dependent on local temperature, pressure and air flow. Although a 'refraction coefficient' of 0.13 is widely used in GIS viewshed analyses (Yoeli 1985: 92), the results of experiments show that this coefficient can vary considerably (see Horyzonty 2024). Rather than accept the 'standard' coefficient uncritically, our approach to this problem moving forward will be to add pressure and temperature as inputs to our model, and a refraction coefficient as a dimension in its output. Experimenting with different coefficients by using satellite temperature and pressure datasets to accurately simulate refraction is the next logical step in the development of our model, which is available on GitHub (see Smith 2026). Ultimately, we see the visibility datasets that we have produced as a first draft that will be updated as better methods are developed. In the meantime, the results presented here can help researchers develop more nuanced questions about seafaring, navigation and visibility; and our method and scripts can give them the tools that they need to answer those questions.

Acknowledgements

Thanks to Julia Kotthaus for help with translations.

Funding statement

This research was funded by Augmentum (www.augmentum.ch) as part of The Practical Mariner Project at the University of Oxford.

Data availability statement

Updated versions of the scripts used in this analysis can be found on Zenodo (Smith 2026). Visibility datasets produced for this analysis are included as online supplementary materials.

Online supplementary material (OSM)

To view supplementary material for this article, please visit https://doi.org/10.15184/aqy.2026.10340 and select the supplementary materials tab.

References

Aubet, M.E. 2001. *The Phoenicians and the West: politics, colonies and trade*. Cambridge: Cambridge University Press.

Benedikt, M.L. 1979. To take hold of space: isovists and isovist fields. *Environment and Planning B: Urban Analytics and City Science* 6: 47–65. https://doi.org/10.1068/b060047

Bernardini, W. *et al.* 2013. Quantifying visual prominence in social landscapes. *Journal of Archaeological Science* 40: 3946–54. https://doi.org/10.1016/j.jas.2013.05.019

BOWEN, E.G. 1970. Britain and the British Seas, in D. Moore (ed.) *The Irish Sea province in archaeology and history*: 13–28. Cardiff: Cambrian Archaeological Association.

BROODBANK, C. 2000. *An island archaeology of the early Cyclades*. Cambridge: Cambridge University Press.

– 2015. *The making of the Middle Sea: a history of the Mediterranean from the beginning to the emergence of the Classical World*. London: Thames and Hudson.

BRUGHMANS, T. *et al.* 2018. Introducing visual neighbourhood configurations for total viewsheds. *Journal of Archaeological Science* 96: 14–25. https://doi.org/10.1016/j.jas.2018.05.006

CALVO-TRIAS, M. & A. GALMÉS-ALBA. 2025. Watching the horizon: coastal navigation strategies in the Balearic archipelago during the Middle and Late Bronze Ages. *Journal of Island and Coastal Archaeology* 20: 259–94. https://doi.org/10.1080/15564894.2024.2307370

CHAPMAN, R. 1990. *Emerging complexity: the later prehistory of south-east Spain, Iberia and the West Mediterranean* (New Studies in Archaeology). Cambridge: Cambridge University Press.

ČUČKOVIĆ, Z. 2016. Advanced viewshed analysis: a Quantum GIS plug-in for the analysis of visual landscapes. *Journal of Open Source Software* 1. https://doi.org/10.21105/joss.00032

– 2018. Land visibility in the Mediterranean: a large scale model. *Landscape Archaeology*. Available at: https://landscapearchaeology.org/2018/mediterranean-land-visibility/ (accessed 17 July 2025).

CUNLIFFE, B. 2008. *Europe between the oceans: themes and variations: 9000 BC–AD 1000*. New Haven (CT): Yale University Press.

– 2017. *On the ocean: the Mediterranean and the Atlantic from prehistory to AD 1500*. Oxford: Oxford University Press.

DANIELSON, J.J. & D.B. GESCH. 2011. Global multi-resolution terrain elevation data 2010 (GMTED2010). Open-File Report 1073. Reston (VA): U.S. Department of the Interior / U.S. Geological Survey. https://doi.org/10.3133/ofr20111073

FISHER, P.F. 1993. Algorithm and implementation uncertainty in viewshed analysis. *International Journal of Geographical Information Systems* 7: 331–47. https://doi.org/10.1080/02693799308901965

GILLINGS, M. 2009. Visual affordance, landscape, and the megaliths of Alderney. *Oxford Journal of Archaeology* 28: 335–56. https://doi.org/10.1111/j.1468-0092.2009.00332.x

GUSTAS, R. & K. SUPERNANT. 2017. Least cost path analysis of early maritime movement on the Pacific Northwest Coast. *Journal of Archaeological Science* 78: 40–56. https://doi.org/10.1016/j.jas.2016.11.006

HENKEL, L. 1901. Grenze der Sichtbarkeit des Landes auf dem Mittelmeer. *Dr. A. Petermanns Mitteilungen aus Justus Perthes' geographischer Anstalt* 47: 284–85.

HIGUCHI, T. 1983. *The visual and spatial structure of landscapes*. Cambridge: Massachusetts Institute of Technology Press.

HÖCKMANN, O. 2005. Schiffahrt im östlichen Mittelmeer im 2. Jt. v. Chr., in Ü. Yalçin *et al.* (ed.) *Das Schiff von Uluburun: Welthandel vor 3000 Jahren: Katalog der Ausstellung des Deutschen Bergbau-Museums Bochum vom 15. Juli 2005 bis 16. Juli 2006* (Veröffentlichungen aus dem Deutschen Bergbau-Museum Bochum 138): 309–24. Bochum: Deutsches Bergbau-Museum.

HORDEN, P. & N. PURCELL. 2000. *The corrupting sea: a study of Mediterranean history*. Oxford: Blackwell.

HORYZONTY, D. 2024. Atmospheric refraction. Available at: https://dalekiehoryzonty.pl/refrakcja-atmosferyczna/ (accessed 25 June 2025).

INMAN, J. 1920. *Nautical tables designed for the use of British seamen*. England: Trübner & Co.

JERLOV, N.G. 1976. *Marine optics* (Elsevier Oceanography Series 14). Amsterdam: Elsevier Scientific.

JERPÅSEN, G.B. 2009. Application of visual archaeological landscape analysis: some results. *Norwegian Archaeological Review* 42: 123–45. https://doi.org/10.1080/00293650903351052

LEHNER, B. *et al.* 2008. New global hydrography derived from spaceborne elevation data. *Eos* 89: 93–94. https://doi.org/10.1029/2008EO100001

LLOBERA, M. 2003. Extending GIS-based visual analysis: the concept of visualscapes. *International Journal of Geographical Information*

Science 17: 25–48. https://doi.org/10.1080/713811741

LONERGAN, C. & N. HEDLEY. 2016. Unpacking isovists: a framework for 3D spatial visibility analysis. *Cartography and Geographic Information Science* 43: 87–102. https://doi.org/10.1080/15230406.2015.1065761

MANNING, S. & L. HULIN. 2005. Maritime commerce and geographies of mobility in the Late Bronze Age of the eastern Mediterranean: problematizations, in E. Blake & A.B. Knapp (ed.) *The archaeology of Mediterranean prehistory*: 270–302. Malden (MA): Blackwell.

MAURO, C.M. & F. DURASTANTE. 2023. Nocturnal seafaring: the reduction of visibility at night and its impact on ancient Mediterranean seafaring. A study based on 8–4th centuries BC evidence. *Journal of Maritime Archaeology* 18: 733–51. https://doi.org/10.1007/s11457-023-09385-0

MCGRAIL, S. 1998. *Ancient boats in north-west Europe: the archaeology of water transport to AD 1500* (Longman Archaeology Series). London: Longman.

MEDAS, S. 2004. *De rebus nauticis: l'arte della navigazione nel mondo antico* (Forma Conventus Tarraconensis. Serie Studia Archaeologica 132). Roma: L'Erma di Bretschneider.

NEUMANN, K. & J. PARTSCH. 1885. *Physikalische Geographie von Griechenland mit besonderer Rücksicht auf das Alterthum*. Breslau: W. Koebner.

POUNCETT, J. 2013. Expanding horizons: visibility, monuments and topography, presented at *Across space and time. Papers from the 41st Annual Conference of Computer Applications and Quantitative Methods in Archaeology, Perth, 25–28 March 2013*.

REW, R. & G. DAVIS. 1990. NetCDF: an interface for scientific data access. *IEEE Computer Graphics and Applications* 10: 76–82. https://doi.org/10.1109/38.56302

SCHÜLE, W. 1970. Navegación primitiva y visibilidad de la tierra en el Mediterráneo, in *XI Congreso Nacional de Arqueología, Mérida, 1968* (Cronica del XI Congreso Arqueológico Nacional): 449–60. Zaragoza: Universidad de Zaragoza.

– 1980. *Orce und Galera: zwei Siedlungen aus dem 3 bis 1. Jahrtausend v. Chr. im Südosten der Iberischen Halbinsel*. Mainz am Rhein: P. von Zabern.

TARTARON, T.F. 2013. *Maritime networks in the Mycenaean world*. Cambridge: Cambridge University Press.

SMITH, K. 2026. polikala62/radial-array-tools: radial-array-tools, version 0.1.0.alpha. Zenodo. https://doi.org/10.5281/zenodo.18621693

VERNET, J. 1978. La Navegación en la Alta Edad Media, in Centro italiano di studi sull'alto Medioevo (ed.) *La navigazione mediterranea nell'alto Medioevo: 14–20 aprile 1977* (Settimane di Studio del Centro Italiano di Studi sull'alto Medioevo 25): 323–81. Spoleto: Presso la Sede del Centro.

WHEATLEY, D. & M. GILLINGS. 2000. Vision, perception and GIS, in G. Lock (ed.) *Beyond the map: archaeology and spatial technologies*: 1–27. Amsterdam: IOS Press.

World Meteorological Organization. 2009. *Manual on codes: international codes*. Geneva: Secretariat of the World Meteorological Organization.

YOELI, P. 1985. The making of intervisibility maps with computer and plotter. *Cartographica* 22: 88–103. https://doi.org/10.3138/J275-6460-8326-3733